Pergamon

Int. J. Heat Mass Transfer Vol. 37, No. 10, pp. 1525–1533, 1994

0017-9310/94 $7.00+0.00

0017-9310(93)F0088-X

Analytical solutions of flow and heat transfer in a porous structure with partial heating and evaporation on the upper surface

YIDING CAO and AMIR FAGHRI

Department of Mechanical and Materials Engineering, Wright State University, Dayton, OH 45435, U.S.A.

(*Received* 9 *February* 1993 *and in final form* 12 *November* 1993)

Abstract—A porous structure with partial heating and evaporation on the upper surface is studied analytically. The liquid pressure and velocities are obtained by solving a Laplace-type equation for the porous structure. A perturbation method is applied for the temperature distribution with higher heat inputs, which consists of zeroth-order solution and a temperature correction. For the temperature correction, an approximate solution is derived using an integral formulation. The analytical solution obtained is useful for the evaporator performance and design of capillary pumped loops.

INTRODUCTION

A CAPILLARY porous structure with partial heating and evaporation on the upper surface is shown in Fig. 1. The entire porous structure is saturated with liquid from the bottom ($y = 0$), which is connected to a pool for the liquid supply. Heat is applied over part of the upper surface ($0 < x < L_{xf}$) which is impermeable to the fluid. The rest of the upper surface ($L_{xf} < x < L_x$) exposes liquid in the pores of the capillary structure to the vapor space above. Heat is transferred from the upper surface ($0 \leqslant x \leqslant L_{xf}$) to the liquid–vapor interface where evaporation takes place. The side walls ($x = 0$ and L_x) are adiabatic and impermeable. The liquid is drawn from the bottom of the porous structure and flows to the liquid–vapor interface due to evaporation.

The porous structure described above is directly related to the evaporator of capillary pumped loops (CPL). A capillary pumped loop has the advantage of transporting large amounts of heat over long distances [1–3]. A commonly encountered problem is that sufficient capillary pressures cannot be developed at the evaporator during operation, which is needed to circulate the working fluid through the CPL. As a result, a two-phase accumulator or mechanical pump is often needed to assist the CPL operation. One of the major causes of this problem is the boiling limitation which occurs in the porous structure of the evaporator. Due to the special geometry of the CPL evaporator, the boiling limitation is more likely to occur than in conventional heat pipes, which largely depends on the temperature distribution in the porous wick, especially at the wick/cover-plate interface. Also, it is important to calculate the pressure drop in the wick structure for the capillary limit consideration.

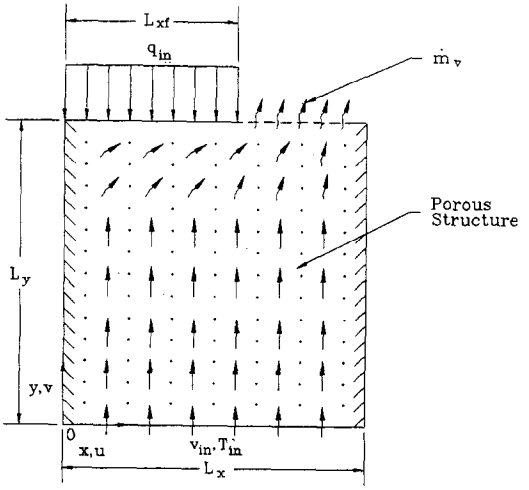

FIG. 1. Porous structure with partial heating and evaporation on the upper surface.

Liquid flow and heat transfer in the CPL is a very complicated process which generally requires numerical simulations. Although the numerical simulation has the advantages of being comprehensive and general, the numerical coding is time-consuming and the application of the numerical results is sometimes difficult. On the other hand, a simple, approximate analytical solution is ready to use and is more convenient for the CPL design. For this reason, approximate analytical solutions are obtained in the present paper for the temperature distribution in the porous structure. With this information, the boiling limitation for the CPL can be determined. For most cases, a two-dimensional model is appropriate for the temperature distribution in the porous wick at the steady state. Also, the temperature drop in the cover plate can be neglected due to its high thermal conductivity. Due to symmetry, a segment of the flat-plate evaporator can

NOMENCLATURE

a_1	constant in equation (38)
a_2	constant in equation (38)
c_p	specific heat [J kg^{-1} K^{-1}]
h_{fg}	latent heat of evaporation [J kg^{-1}]
k	thermal conductivity [W m^{-1} K^{-1}]
k_{eff}	effective thermal conductivity, equation (6) [W m^{-1} K^{-1}]
K	wick permeability [m^2]
L_x	total length in x direction [m]
L_y	total length in y direction [m]
L_{xf}	heating length on the upper surface [m]
$\dot{m}_v$	vapor mass flux due to evaporation [kg m^{-2} s^{-1}]
p	liquid pressure [N m^{-2}]
Pr	Prandtl number, ν_l/α_{eff}
q	heat flux [W m^{-2}]
Re	Reynolds number, $v_{in}L_x/\nu_l$
$\bar{S}$	integral in equation (40)
s	source term in equation (37)
T	temperature [K]
T_1	temperature correction [K]
T_0	zeroth-order temperature [K]
T^+	temperature difference, $T-T_{in}$ [K]
u	liquid velocity in x direction [m s^{-1}]
u^+	dimensionless velocity in x direction $[u/v_{in}]$
v	liquid velocity in y direction [m s^{-1}]
v^+	dimensionless velocity in y direction $[v/v_{in}]$
x, y	coordinates [m]
x^+, y^+	dimensionless coordinates, $(x/L_x)/(RePr)$, $(y/L_x)/(RePr)$.

Greek symbols

α	thermal diffusivity [m^2 s^{-1}]
ν_l	liquid kinematic viscosity [m^2 s^{-1}]
ρ	density [kg m^{-3}]
φ	porosity.

Subscripts

eff	effective
i	wick–vapor interface or initial condition
in	inlet
l	liquid working fluid in the porous structure
out	outlet
s	solid matrix
v	vapor.

be studied. Therefore, a flat-plate CPL evaporator can be simplified to the situation shown in Fig. 1.

MATHEMATICAL FORMULATION

For the liquid flow in the porous structure, Darcy's law is applied [4]:

$$u = \frac{K}{\mu}\left(-\frac{\partial p}{\partial x}\right) \tag{1}$$

$$v = \frac{K}{\mu}\left(-\frac{\partial p}{\partial y}\right) \tag{2}$$

where K is the wick permeability, and u and v are the area-averaged fluid velocities. The corresponding continuity equation is

$$\frac{\partial u}{\partial x} + \frac{\partial v}{\partial y} = 0. \tag{3}$$

The energy equation for the porous wick is

$$u\frac{\partial T}{\partial x} + v\frac{\partial T}{\partial y} = \alpha_{eff}\left(\frac{\partial^2 T}{\partial x^2} + \frac{\partial^2 T}{\partial y^2}\right). \tag{4}$$

The effective thermal diffusivity α_{eff} is defined as

$$\alpha_{eff} = k_{eff}/\rho_l c_{pl} \tag{5}$$

where

$$k_{eff} = \varphi k_l + (1-\varphi)k_s \tag{6}$$

which is an aggregate property of the fluid-saturated porous medium. $(\rho_l c_{pl})$ is a property of the fluid only, and φ is the wick porosity. In the above formulation, it is assumed that the porous structure is homogeneous and isotropic. It is also assumed that the solid matrix is in local thermal equilibrium with the fluid filling the pores, and the order of the local Reynolds number based on the average velocity and $K^{1/2}$ does not exceed unity.

The boundary conditions are:

$x = 0$ and $x = L_x$:

$$u = 0, \quad \frac{\partial T}{\partial x} = 0 \tag{7}$$

$y = 0$:

$$v = v_{in}, \quad T = T_{in} \tag{8}$$

$y = L_y$ and $0 \leqslant x \leqslant L_{xf}$:

$$v = 0, \quad k_{eff}\frac{\partial T}{\partial y} = q_{in} \tag{9}$$

$y = L_y$ and $L_{xf} < x < L_x$:

$$v = v_{out}, \quad k_{eff}\frac{\partial T}{\partial y} = -(\rho v)_{out}h_{fg} = -q_{out}. \tag{10}$$

ANALYTICAL SOLUTION OF THE LIQUID FLOW

Combining equations (1)–(3), a Laplace-type equation is obtained [4]:

$$\frac{\partial^2 p}{\partial x^2}+\frac{\partial^2 p}{\partial y^2}=0 \tag{11}$$

with boundary conditions:

$x=0$ and $x=L_x$:

$$\frac{\partial p}{\partial x}=0 \tag{12}$$

$y=0$:

$$\frac{\partial p}{\partial y}=-\frac{\mu}{K}v_{in} \tag{13}$$

$y=L_y$:

$$\frac{\partial p}{\partial y}=\begin{cases}0 & (0\leqslant x\leqslant L_{xf})\\ -\mu v_{out}/K & (L_{xf}<x\leqslant L_x)\end{cases}. \tag{14}$$

Equations (11)–(14) can be solved by the method of separation of variables [5]. The solution thus obtained is

$$p(x,y)=C_o-\frac{\mu}{K}v_{in}y+\sum_{m=1}^{\infty}\frac{2L_x(\mu v_{out}/K)}{(m\pi)^2}\times\frac{\sin\left(\frac{m\pi}{L_x}L_{xf}\right)}{\sinh\left(\frac{m\pi}{L_x}L_y\right)}\cosh\left(\frac{m\pi y}{L_x}\right)\cos\left(\frac{m\pi x}{L_x}\right)$$

$$=C_o-\frac{\mu}{K}v_{in}y+\sum_{m=1}^{\infty}\frac{2L_x(\mu v_{out}/K)}{(m\pi)^2}\times\sin\left(\frac{m\pi L_{xf}}{L_x}\right)\cos\left(\frac{m\pi x}{L_x}\right)\times\frac{\exp\left[-\frac{m\pi}{L_x}(L_y-y)\right]+\exp\left[-\frac{m\pi}{L_x}(L_y+y)\right]}{1-\exp\left[-2\frac{m\pi}{L_x}L_y\right]} \tag{15}$$

where C_o is an arbitrary constant. Due to the boundary conditions given in equations (12)–(14), the pressure gradients are meaningful, but the absolute value of the pressure is not meaningful. The velocities are obtained by combining equations (1), (2), and (15).

$$v=v_{in}-\sum_{m=1}^{\infty}\frac{2v_{out}}{m\pi}\sin\left(\frac{m\pi L_{xf}}{L_x}\right)\cos\left(\frac{m\pi}{L_x}x\right)\times\frac{\exp\left[-\frac{m\pi}{L_x}(L_y-y)\right]-\exp\left[-\frac{m\pi}{L_x}(L_y+y)\right]}{1-\exp\left[-2\frac{m\pi}{L_x}L_y\right]} \tag{16}$$

$$u=\sum_{m=1}^{\infty}\frac{2v_{out}}{m\pi}\sin\left(\frac{m\pi L_{xf}}{L_x}\right)\sin\left(\frac{m\pi}{L_x}x\right)\times\frac{\exp\left[-\frac{m\pi}{L_x}(L_y-y)\right]+\exp\left[-\frac{m\pi}{L_x}(L_y+y)\right]}{1-\exp\left[-2\frac{m\pi}{L_x}L_y\right]}. \tag{17}$$

ANALYTICAL SOLUTION OF THE ENERGY EQUATION

The energy equation as well as the boundary conditions are given by equations (4)–(10). By introducing the following parameters,

$$x^+=\frac{x/L_x}{RePr},\quad y^+=\frac{y/L_x}{RePr},\quad u^+=\frac{u}{v_{in}},$$

$$v^+=\frac{v}{v_{in}},\quad T^+=T-T_{in},$$

$$Re=\frac{v_{in}L_x}{\nu_l},\quad Pr=\frac{\nu_l}{\alpha_{eff}} \tag{18}$$

the energy equation is transformed into

$$\frac{\partial^2 T^+}{\partial x^{+2}}+\frac{\partial^2 T^+}{\partial y^{+2}}=\left(u^+\frac{\partial T^+}{\partial x^+}+v^+\frac{\partial T^+}{\partial y^+}\right)(RePr)^2. \tag{19}$$

From equation (18), the parameter $RePr$ is a combination of properties of the working fluid and the wick structure, which can be expressed as

$$RePr=\frac{v_{in}L_x}{\nu_l}\frac{\nu_l}{\alpha_{eff}}=\frac{\rho_l v_{in}L_x c_{pl}}{k_{eff}}. \tag{20}$$

By making an energy balance over the whole porous structure, we have

$$q_{in}L_{xf}+\left(-k_{eff}\left.\frac{\partial T}{\partial y}\right|_{y=0}\right)L_x+v_{in}\rho_l c_{pl}T_{in}L_x=v_{out}\rho_l h_{fg}(L_x-L_{xf})+v_{out}\rho_l c_{pl}T_{out}(L_x-L_{xf}) \tag{21}$$

where T_{out} is the average temperature at the liquid–vapor interface. Considering the mass balance

$$v_{in}\rho_l L_x=v_{out}\rho_l(L_x-L_{xf}) \tag{22}$$

and substituting equation (22) into equation (21), we have

$$q_{in}L_{xf}=v_{in}\rho_l L_x h_{fg}+\left(k_{eff}\left.\frac{\partial T}{\partial y}\right|_{y=0}\right)L_x+v_{in}\rho_l c_{pl}L_x(T_{out}-T_{in}).$$

The sensible heat term in the above equation is much smaller than the latent heat term, and can be neglected.

$$q_{in}L_{xf} = v_{in}\rho_l L_x h_{fg} + \left(k_{eff}\frac{\partial T}{\partial y}\bigg|_{y=0}\right)L_x. \quad (23)$$

Therefore,

$$Re\,Pr = \frac{\rho_l v_{in} L_x c_{pl}}{k_{eff}} = \left(q_{in}L_{xf} - L_x k_{eff}\frac{\partial T}{\partial y}\bigg|_{y=0}\right)c_{pl}/(h_{fg}k_{eff}). \quad (24)$$

As a first approximation, neglect the heat flux at $y = 0$.

$$Re\,Pr = \frac{\rho_l v_{in} L_x c_{pl}}{k_{eff}} \approx \frac{q_{in}L_{xf}}{h_{fg}}\frac{c_{pl}}{k_{eff}}. \quad (25)$$

The parameter $Re\,Pr$ is usually very small. For a CPL evaporator with heat input and thermal properties of $q_{in} = 10^4$ W m^{-2}, $L_{xf} = 0.5$ mm, $c_{pl} = 2.0\times10^3$ J kg^{-1} K^{-1}, $h_{fg} = 2.0\times10^5$ J kg^{-1}, and $k_{eff} = 4.0$ W m^{-1} K^{-1}, $RePr$ is on the order of 10^{-2}. Therefore, for a small or moderate heat input, the term on the right-hand side of equation (19) can be neglected. For $RePr = 0$, equation (19) becomes

$$\frac{\partial^2 T_0^+}{\partial x^{+2}} + \frac{\partial^2 T_0^+}{\partial y^{+2}} = 0 \quad (26)$$

with boundary conditions

$x^+ = 0$ and L_x^+:

$$\frac{\partial T_0^+}{\partial x^+} = 0 \quad (27)$$

$y^+ = 0$:

$$T_0^+ = 0 \quad (28)$$

$y^+ = L_y^+$ and $0 \leqslant x^+ \leqslant L_{xf}^+$:

$$\frac{\partial T_0^+}{\partial y^+} = \frac{L_x\,Re\,Pr\,q_{in}}{k_{eff}} \quad (29)$$

$y^+ = L_y^+$ and $L_{xf}^+ < x^+ \leqslant L_x^+$:

$$\frac{\partial T_0^+}{\partial y^+} = -\frac{L_x\,Re\,Pr\,q_{out}}{k_{eff}}. \quad (30)$$

The solution to the above equation and boundary conditions is obtained by the method of separation of variables.

$$T_0^+(x^+,y^+) = \sum_{m=1}^{\infty}\frac{2L_x(q_{in}+q_{out})\sin\left(\frac{m\pi}{L_x^+}L_{xf}^+\right)}{(m\pi)^2 k_{eff}} \times \frac{\sinh\left(\frac{m\pi}{L_x^+}y^+\right)}{\cosh\left(\frac{m\pi}{L_x^+}L_y^+\right)}\cos\left(\frac{m\pi}{L_x^+}x^+\right)$$

$$= \sum_{m=1}^{\infty}\frac{2L_x(q_{in}+q_{out})}{(m\pi)^2 k_{eff}}\sin\left(\frac{m\pi}{L_x^+}L_{xf}^+\right)\cos\left(\frac{m\pi}{L_x^+}x^+\right) \times \frac{\exp\left[-\frac{m\pi}{L_x^+}(L_y^+ - y^+)\right] - \exp\left[-\frac{m\pi}{L_x^+}(L_y^+ + y^+)\right]}{1+\exp\left(-2\frac{m\pi}{L_x^+}L_y^+\right)}. \quad (31)$$

For $Re\,Pr \neq 0$, an exact analytical solution is not available. Since $Re\,Pr$ is a small number, a perturbation method can be used [6]. The solution for $RePr \neq 0$ can be expressed as

$$T^+(x^+,y^+) = T_0^+(x^+,y^+) + (Re\,Pr)^2 T_1^+(x^+,y^+) \quad (32)$$

where $T_0^+(x^+, y^+)$ is the solution with $RePr = 0$, and $T_1^+(x^+, y^+)$ is the first-order solution associated with $(Re\,Pr)^2$. The terms with higher order of $Re\,Pr$ have been neglected due to the very small value of $Re\,Pr$. Substituting equation (32) into equation (19), and collecting the terms associated with $(RePr)^2$, we have

$$\frac{\partial^2 T_1^+}{\partial x^{+2}} + \frac{\partial^2 T_1^+}{\partial y^{+2}} = u^+\frac{\partial T_0^+}{\partial x^+} + v^+\frac{\partial T_0^+}{\partial y^+} \quad (33)$$

with boundary conditions

$x^+ = 0$ and $x^+ = L_x^+$:

$$\frac{\partial T_1^+}{\partial x^+} = 0 \quad (34)$$

$y^+ = 0$:

$$T_1^+ = 0 \quad (35)$$

$y^+ = L_y^+$:

$$\frac{\partial T_1^+}{\partial y^+} = 0. \quad (36)$$

Since the solutions for T_0^+ and the velocities u^+ and v^+ have been already obtained, the term on the right-hand side of equation (33) is a source term.

$$s(x^+,y^+) = u^+\frac{\partial T_0^+}{\partial x^+} + v^+\frac{\partial T_0^+}{\partial y^+}. \quad (37)$$

However, this source term is a very complex function of x^+ and y^+ due to the multiplication of the infinite series for T_0^+, u^+, and v^+. In general, numerical computations are needed to solve the equation. Since the equation is basically a heat-conduction type equation, minimal numerical efforts are required for this problem. However, since the primary objective of this study is to obtain analytical closed-form solutions, an approximate method is applied. The solution for T_1^+ is approximated by the following relation.

$$T_1^+ = \frac{(3L_y^{+2}y^+ - y^{+3})}{2L_y^{+3}}\left[a_1 + a_2\left(\frac{L_x^{+2} - x^{+2}}{L_x^{+2}}\right)^2\right]. \quad (38)$$

The above equation satisfies the boundary conditions for T_1^+, equations (34)–(36). a_1 and a_2 are constants to be determined. In this study, the integral formulation is applied to determine the constants. The differential equation (33) is integrated over the porous structure.

$$\int_0^{L_y^+}\int_0^{L_x^+}\left(\frac{\partial^2 T_1^+}{\partial x^{+2}}+\frac{\partial^2 T_1^+}{\partial y^{+2}}\right)\mathrm{d}x^+\,\mathrm{d}y^+ = \int_0^{L_y^+}\int_0^{L_y^+}\left(u^+\frac{\partial T_0^+}{\partial x^+}+v^+\frac{\partial T_0^+}{\partial y^+}\right)\mathrm{d}x^+\,\mathrm{d}y^+. \quad (39)$$

Using the continuity equation (3), and the boundary conditions for u^+, v^+, and T_0^+ (equations (7), (9), (10), and (28)), the integral source term on the right-hand side of equation (39) is

$$\begin{aligned}\bar{S} &= \int_0^{L_y^+}\int_0^{L_x^+}\left(u^+\frac{\partial T_0^+}{\partial x^+}+v^+\frac{\partial T_0^+}{\partial y^+}\right)\mathrm{d}x^+\,\mathrm{d}y^+\\ &= \int_0^{L_y^+}\int_0^{L_x^+}\left[\frac{\partial(u^+T_0^+)}{\partial x^+}+\frac{\partial(v^+T_0^+)}{\partial y^+}\right]\mathrm{d}x^+\,\mathrm{d}y^+\\ &= \int_0^{L_y^+} v^+(x^+,L_y^+)\,T_0^+(x^+,L_y^+)\,\mathrm{d}x^+\\ &= v_{\text{out}}^+\int_{L_{xf}^+}^{L_x^+} T_0^+(x^+,L_y^+)\,\mathrm{d}x\\ &= -v_{\text{out}}^+\sum_{m=1}^{\infty}\frac{2L_x(q_{\text{in}}+q_{\text{out}})\sin^2\left(\frac{m\pi}{L_x^+}L_{xf}^+\right)}{\left[\frac{(m\pi)^3}{L_x^+}\right]k_{\text{eff}}\cosh\left(\frac{m\pi}{L_x^+}L_y^+\right)}\\ &\quad\times\sinh\left(\frac{m\pi}{L_x^+}L_y^+\right). \end{aligned} \quad (40)$$

For the left-hand side of equation (39), applying boundary conditions (34)–(36) gives

$$\int_0^{L_y^+}\int_0^{L_x^+}\left(\frac{\partial^2 T_1^+}{\partial x^{+2}}+\frac{\partial^2 T_1^+}{\partial y^{+2}}\right)\mathrm{d}x^+\,\mathrm{d}y^+ = \int_0^{L_x^+}-\left.\frac{\partial T_1^+}{\partial y^+}\right|_{y^+=0}\mathrm{d}x^+. \quad (41)$$

Combining equations (38)–(41), a_1 is obtained as

$$a_1 = -\frac{2}{3}\frac{L_y^+}{L_x^+}\bar{S}-\frac{8}{15}a_2. \quad (42)$$

Another condition used to determine the constants is that, at some specific points, the differential equation is satisfied. Since the highest temperature will occur at the left upper corner of the porous structure, the approximate relation is imposed to satisfy the differential governing equation at that point.

$$\frac{\partial^2 T_1^+}{\partial x^{+2}}+\frac{\partial^2 T_1^+}{\partial y^{+2}} = u^+\frac{\partial T_0^+}{\partial x^+}+v^+\frac{\partial T_0^+}{\partial y^+},$$
$$\text{at } x^+ = 0 \text{ and } y^+ = L_y^+. \quad (43)$$

Substituting equation (38) into equation (43) results in

$$a_1 = -\left(1+\frac{4}{3}\frac{L_y^{+2}}{L_x^{+2}}\right)a_2. \quad (44)$$

From equations (42) and (44), a_1 and a_2 are

$$a_1 = -\frac{(40L_y^{+3}+30L_y^+L_x^{+2})\bar{S}}{21L_x^{+3}+60L_x^+L_y^{+2}} \quad (45)$$

$$a_2 = \frac{10L_y^+L_x^+\bar{S}}{7L_x^{+2}+20L_y^{+2}}. \quad (46)$$

Therefore,

$$\begin{aligned}T_1^+(x^+,y^+) &= \left(\frac{3L_y^{+2}y^+-y^{+3}}{2L_y^{+3}}\right)\\ &\quad\times\left[-\frac{(40L_y^{+3}+30L_y^+L_x^{+2})\bar{S}}{21L_x^{+3}+60L_x^+L_y^{+2}}\right.\\ &\quad\left.+\frac{10L_y^+L_x^+\bar{S}}{7L_x^{+2}+20L_y^{+2}}\left(\frac{L_x^{+2}-x^{+2}}{L_x^{+2}}\right)^2\right]. \end{aligned} \quad (47)$$

The above approximate relation is not the only one that may be derived for equations (33)–(36). In fact, for a particular problem, one approximation may be more convenient than another. The choice depends on experience, the accuracy required in the solution, and the complexity of the problem. The above solution can be improved at the cost of an involved analysis. However, since T_1^+ is associated with $(Re\,Pr)^2$, its contribution to T^+ is usually small, so an approximate relation with reasonable accuracy is acceptable.

RESULTS AND DISCUSSION

Figure 2 presents the dimensionless liquid velocity vectors in the porous structure, which were obtained analytically from equations (16) and (17). The geometry parameters and thermal properties for this case are: $L_x = 0.75$ mm, $L_y = 0.75$ mm, $L_{xf} = 0.5$ mm, $k_{\text{eff}} = 4$ W m^{-1} K^{-1}, $c_{\text{pl}} = 2\times10^3$ J kg^{-1} K^{-1}, $h_{\text{fg}} = 2\times10^5$ J kg^{-1} and $q_{\text{in}} = 2\times10^4$ W m^{-2}. As a first approximation, the heat flux at $y = 0$ is neglected, and equation (25) is used in the calculation of $RePr$. This makes both dimensionless parameters x^+ and y^+ nearly 40. The liquid flows vertically into the porous wick structure at $y^+ = 0$, and remains nearly one-dimensional until reaching the middle section of the porous structure. The liquid flow in the region $0 \leqslant x^+ \leqslant L_{xf}^+$ changes direction due to the upper impermeable boundary and moves toward the liquid–vapor interface region ($L_{xf}^+ < x^+ < L_x^+$).

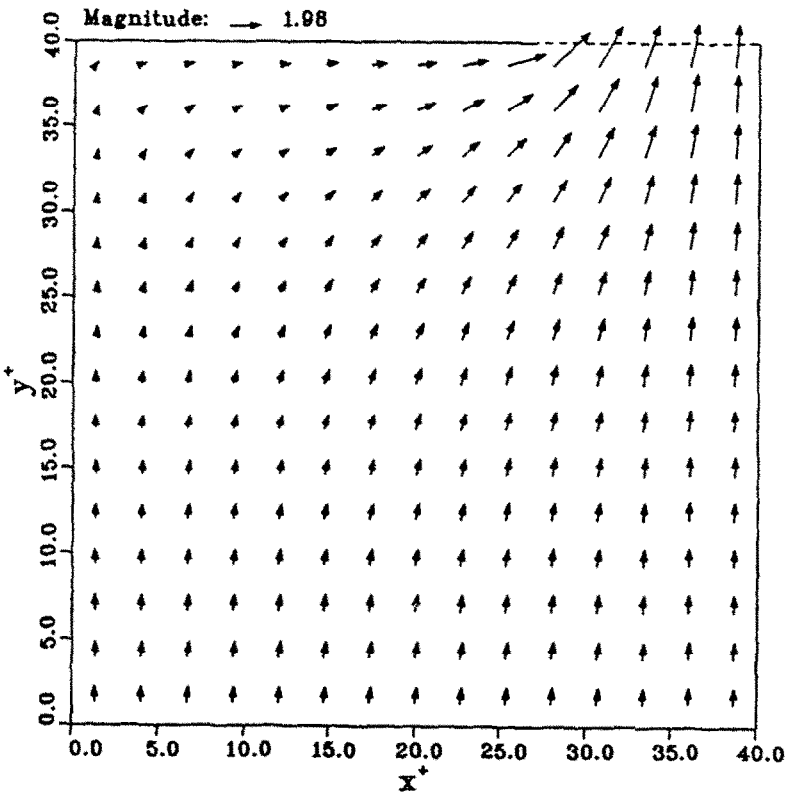

FIG. 2. Dimensionless velocity vectors in the porous wick structure.

In order to check the accuracy of the approximate solution for the temperature correction T_1^+, equation (33) and the boundary conditions (34)–(36) were solved numerically using the control-volume finite difference approach [7]. Numerical and approximate solutions for the temperature correction T_1^+ at $x^+ = 0$ and $y^+ = 0.5L_y^+$ are compared in Fig. 3. The agreement between the two solutions is generally good. In addition, both numerical and approximate temperature correction results were substituted into equation (32), and the temperature solutions for the porous structure thus obtained are compared in Fig. 4. As can be seen, both solutions agree very well, and the discrepancy between the two solutions is much smaller than that of solutions for T_1^+. Since $RePr$ is a very small number, little error from the approximate solution was carried through to the final solution for T^+. q_{out} in the analytical solution is calculated to be $q_{out} = q_{in}L_{xf}/(L_x - L_{xf})$ due to the neglection of heat flux at $y^+ = 0$.

Figure 5 shows temperature contours for T^+ in the wick structure. The maximum temperature occurs at the upper left-hand corner, and gradually decreases to the minimum at the upper right-hand corner. Figure 6 shows analytical T^+ and T_0^+ at $x^+ = 0$ for different heat inputs q_{in}. Both temperatures increase significantly with higher heat input. Also, T^+ departs from T_0^+ when the heat input is high. Since the liquid velocity in the porous structure is directly related to the heat input, a higher heat flux means a higher liquid flow velocity. T_0^+ differs from T^+ in that the convective terms are neglected in the governing equation for T_0^+. A higher T^+ than T_0^+ is due to the liquid flow in the porous structure. For the present porous

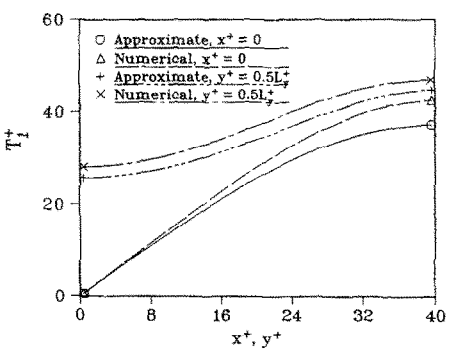

FIG. 3. Comparison of numerical and approximate temperature corrections at $x^+ = 0$ and $y^+ = 0.5L_y^+$.

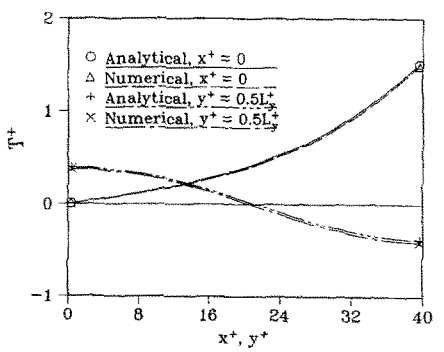

FIG. 4. Comparison between numerical and approximate temperature solutions at $x^+ = 0$ and $y^+ = 0.5L_y^+$.

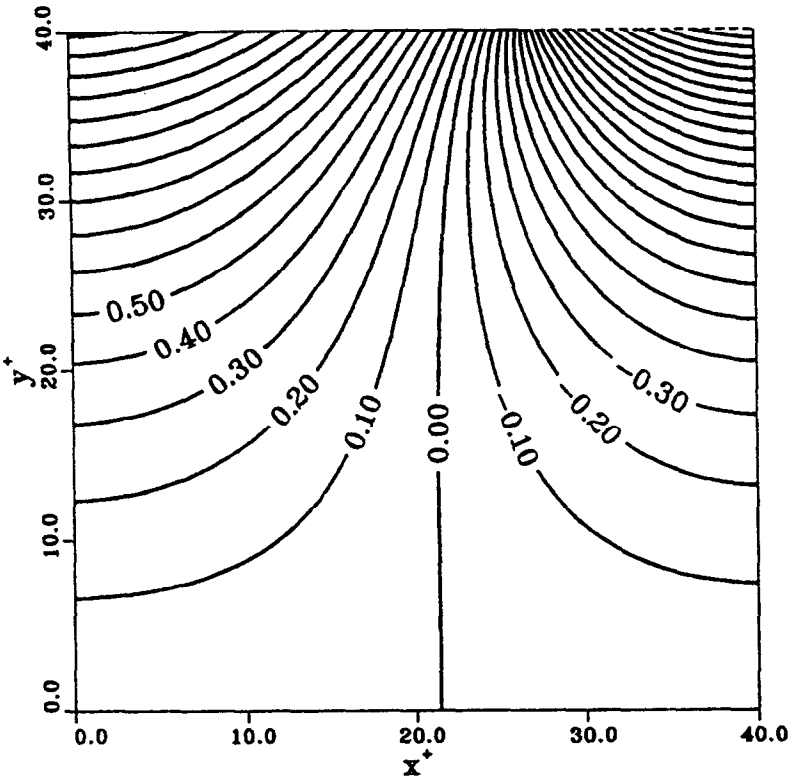

FIG. 5. T^+ isotherms in the porous wick structure.

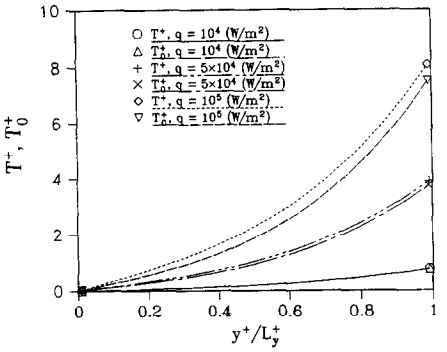

FIG. 6. Analytical T^+ and T_0^+ at $x^+ = 0$ for different q_{in}.

structure, liquid flows upward while heat flows downward in the region close to $x^+ = 0$. The net effect of these two processes is to increase the temperature in this region. Figure 7 shows analytical solutions of T^+ and T_0^+ at $y^+ = L_y^+$ for the same heat fluxes examined in Fig. 6. The temperature T^+ with convective terms is also consistently higher than T_0^+ without convective terms. However, the absolute value of T^+ in the region $L_{xf}^+ < x^+ < L_x^+$ is smaller than that of T_0^+. In this region, heat fluxes begin to change direction, and eventually flow in the same direction as the liquid velocity. As a result, the temperature difference between the inlet and the evaporating liquid–vapor interface is reduced.

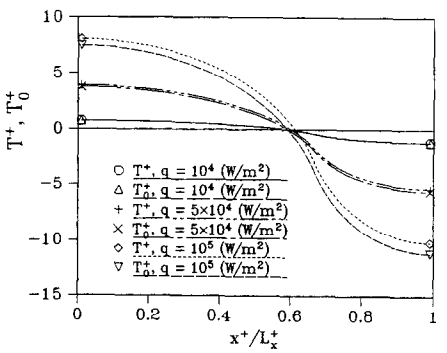

FIG. 7. Analytical T^+ and T_0^+ at $y^+ = L_y^+$ for different q_{in}.

Figure 8 shows the analytical solutions of the temperature T^+ at $x^+ = 0$ and $y^+ = L_y^+$ for different effective thermal conductivities. The effective thermal conductivity has a pronounced effect on the temperature distributions in both directions. As the effective thermal conductivity is reduced, the absolute value of T^+ at the upper surface increases sharply.

For the previous results, the working fluid was con-

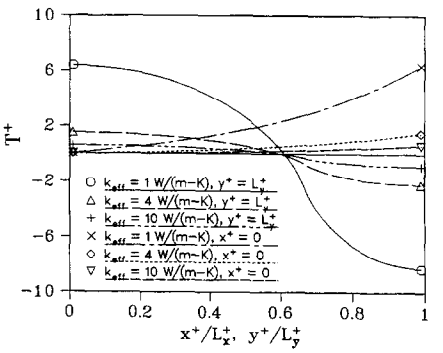

FIG. 8. Analytical T^+ at $y^+ = L_y^+$ and $x^+ = 0$ for different effective thermal conductivities ($q_{in} = 2 \times 10^4$ W m^{-2}).

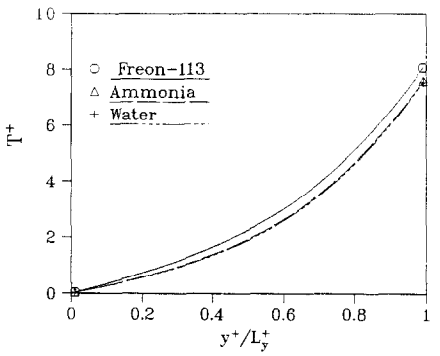

FIG. 9. Analytical T^+ at $x^+ = 0$ for different working fluids ($q_{in} = 10^5$ W m^{-2})

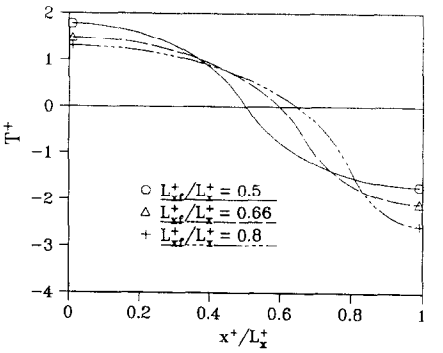

FIG. 11. Analytical solutions of T^+ at $y^+ = L_y^+$ for different geometric parameters ($Q_{in} = 10$ W m^{-1})

sidered to be Freon-113. Figure 9 shows analytical solutions of T^+ at $x^+ = 0$ for different working fluids with $q_{in} = 10^5$ W m^{-2}. The temperature with Freon-113 is relatively higher than that with ammonia or water. For Freon-113, the latent heat of evaporation h_{fg} is on the order of 10^5 J kg^{-1}, while those of ammonia and water are on the order of 10^6 J kg^{-1}. The liquid mass flow rate is directly related to the latent heat, $\dot{m}_l = q_{in}/h_{fg}$. With the same heat input, the liquid mass flow rate for Freon-113 in the porous structure is considerably higher than that for ammonia or water. Therefore, the temperature T^+ for Freon-113 is accordingly higher.

In the above calculations, the heat flux at $y^+ = 0$ has been neglected. In order to validate this assumption, equation (24) is used to calculate $RePr$, in which the heat flux at $y^+ = 0$, $q_o = -k_{eff}(\partial T/\partial y)|_{y=0}$, is obtained by iteration. q_o is first calculated using the solution based on the assumption $q_o = 0$. If $|q_o|$ is zero, the assumption is valid. If $|q_o| \neq 0$, equation (24) is used to calculate $RePr$, and q_{out} is calculated by the energy balance

$$q_{out} = \frac{\left(q_{in}L_{xf} - L_y k_{eff}\left.\frac{\partial T}{\partial y}\right|_{y=0}\right)}{(L_x - L_{xf})}. \quad (48)$$

An analytical solution can be obtained based on the values of $RePr$ and q_{out} given. Then, a new q_o based on this solution is obtained. If the relative difference between the new q_o and previous q_o is greater than 10^{-3}, another iteration is made until the criterion is satisfied. Only a very few iterations are needed for the above procedure, and analytical solutions thus obtained are presented in Fig. 10 at $y^+ = L_y^+$ with different L_y^+/L_x^+, and compared with the corresponding solutions with the assumption of $q_o = 0$. For larger values of L_y^+/L_x^+, the difference between the solutions with and without $q_o = 0$ is negligibly small. For small values of L_y^+/L_x^+, however, large errors may result for the solution based on the assumption $q_o = 0$. For the case of $L_y^+/L_x^+ = 0.6$, more than half of the total heat input is transferred out of the porous structure through the surface $y^+ = 0$.

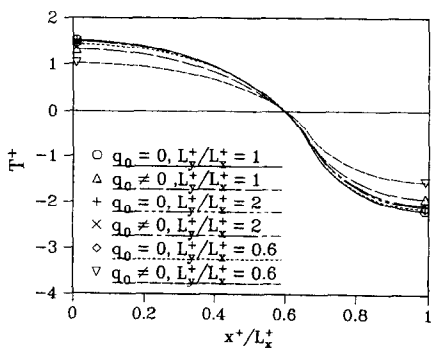

FIG. 10. Comparison of solutions with and without the assumption of $q_0 = 0$ for different geometric parameters at $y^+ = L_y^+$.

Figure 11 presents analytical solutions of T^+ at $y^+ = L_y^+$ from different geometric parameters. The total heat input $Q_{in} = q_{in}L_{xf}$ is held constant at 10 W m^{-1}, L_x is fixed at 0.75 mm, and L_y^+/L_x^+ is kept constant at 1.5. Upon varying L_{xf}^+/L_x^+ from 0.5 to 0.8, it can be seen that the temperature distribution is somewhat sensitive to this parameter, and a small L_{xf}^+/L_x^+ results in a higher temperature at $x^+ = 0$. A smaller L_{xf}^+/L_x^+ in this case means a small L_{xf}. Since the total heat input Q_{in} is kept constant, a small L_{xf} means a higher heat flux in the region $0 < x < L_{xf}$. Therefore, the temperature at $x = 0$ is accordingly higher.

CONCLUSIONS

Analytical solutions for liquid pressures, velocities and temperature in the porous structure were obtained. The approximate solution for the temperature correction was compared with the corresponding numerical results with reasonable agreement. The accuracy of the analytical temperature relation obtained was also examined, and it was shown that the temperature field in the porous structure can be accurately predicted. A parametric study for the porous structure was then presented, and the condition under which the assumption $q_o = 0$ can be made was given. For the thermal design of capillary pumped loops, the boiling limit is one of the primary concerns, which is largely dependent on the highest temperature at the upper left-hand corner of the wick structure. Also, for a given wick structure and working condi-

tions, it is desirable to know the pressure drop over the structure for the capillary limit consideration. The analytical relations obtained in this paper provide a useful tool to deal with these problems.

REFERENCES

1. J. Ku, E. J. Kroliczek and R. McIntosh, Capillary pumped loop technology development, *Proceedings of the Sixth International Heat Pipe Conference*, France (1987).
2. H. Wulz and E. Embacher, Capillary pumped loops for space applications experimental and theoretical studies on the performance of capillary evaporator designs, *Proceedings of the AIAA/ASME 5th Joint Thermophysics and Heat Transfer Conference*, Seattle, WA (1990).
3. J. M. Gottschlich and R. Richter, Thermal power loops, *Proceedings of the SAE Aerospace Atlantic Conference*, Dayton, OH, April (1992).
4. A. Bejan, *Convection Heat Transfer*. Wiley, New York (1984).
5. M. N. Ozisik, *Heat Conduction*. Wiley, New York (1980).
6. C. M. Bender and S. A. Orszag, *Advanced Mathematical Methods for Scientists and Engineers*. McGraw-Hill, New York (1978).
7. S. V. Patankar, *Numerical Heat Transfer and Fluid Flow*. McGraw-Hill, New York (1980).